Neuron
Article

AMPA Receptor Signaling through BRAG2 and Arf6 Critical for Long-Term Synaptic Depression

Ralf Scholz,[1] Sven Berberich,[2] Louisa Rathgeber,[1] Alexander Kolleker,[2] Georg Köhr,[2] and Hans-Christian Kornau[1,*]
[1]Center for Molecular Neurobiology (ZMNH), University of Hamburg, Falkenried 94, D-20251 Hamburg, Germany
[2]Department of Molecular Neurobiology, Max-Planck-Institute for Medical Research, Jahnstraße 29, D-69120 Heidelberg, Germany
*Correspondence: hckornau@zmnh.uni-hamburg.de
DOI 10.1016/j.neuron.2010.05.003

SUMMARY

Central nervous system synapses undergo activity-dependent alterations to support learning and memory. Long-term depression (LTD) reflects a sustained reduction of the synaptic AMPA receptor content based on targeted clathrin-mediated endocytosis. Here we report a current-independent form of AMPA receptor signaling, fundamental for LTD. We found that AMPA receptors directly interact via the GluA2 subunit with the synaptic protein BRAG2, which functions as a guanine-nucleotide exchange factor (GEF) for the coat-recruitment GTPase Arf6. BRAG2-mediated catalysis, controlled by ligand-binding and tyrosine phosphorylation of GluA2, activates Arf6 to internalize synaptic AMPA receptors upon LTD induction. Furthermore, acute blockade of the GluA2-BRAG2 interaction and targeted deletion of BRAG2 in mature hippocampal CA1 pyramidal neurons prevents LTD in CA3-to-CA1 cell synapses, irrespective of the induction pathway. We conclude that BRAG2-mediated Arf6 activation triggered by AMPA receptors is the convergent step of different forms of LTD, thus providing an essential mechanism for the control of vesicle formation by endocytic cargo.

INTRODUCTION

AMPA-type glutamate receptors convey the majority of rapid excitatory neurotransmission in the brain. These ligand-gated, tetrameric ion channels are composed of subunits GluA1–A4 (GluR-A to -D, GluR1–4) with GluA1A2 and GluA2A3 representing the principal synaptic assemblies in CA1 pyramidal neurons (Lu et al., 2009). Trafficking of AMPA receptors (AMPARs) into and out of the postsynaptic membrane, either by lateral diffusion within the plasma membrane or by vesicular transport, supports changes in synaptic strength for learning and memory processes (Derkach et al., 2007; Kessels and Malinow, 2009; Newpher and Ehlers, 2008). The major forms of LTD, which are triggered by NMDA receptor (NMDAR) or metabotropic glutamate receptor (mGluR) activation (Malenka and Bear, 2004), become expressed as a sustained reduction of the synaptic AMPAR content. This is achieved by clathrin-mediated endocytosis and relies on sequences within the intracellular C-terminal region of the GluA2 subunit (GluA2-CT) (Beattie et al., 2000; Lin et al., 2000; Man et al., 2000). A binding site for the clathrin adaptor complex AP2 in GluA2-CT is essential for LTD (Lee et al., 2002; Man et al., 2000), and blockade of AP2 binding in the perirhinal cortex impaired visual recognition memory in rats (Griffiths et al., 2008). In addition, a peptide with a tyrosine-rich sequence motif derived from GluA2-CT blocked LTD and interfered with select cognitive functions in hippocampus (Ahmadian et al., 2004; Wong et al., 2007), nucleus accumbens (Brebner et al., 2005), lateral amygdala (Yu et al., 2008), and medial prefrontal cortex (Van den Oever et al., 2008). Thus, both AP2 binding and an unknown signaling event by the tyrosine-rich sequence of GluA2-CT appear to be required for the expression of LTD in diverse neuronal circuits.

Synaptic plasticity is accompanied by dynamic phosphorylation of the C-terminal regions of AMPAR subunits (Malenka and Bear, 2004), which either changes the open probability or affects trafficking and stabilization of AMPARs at synaptic or extrasynaptic sites (Shepherd and Huganir, 2007). The tyrosine-rich motif of GluA2-CT is also subject to phosphorylation (Ahmadian et al., 2004; Hayashi and Huganir, 2004), but the consequences of this modification remained elusive.

BRAG2/GEP100 is a member of a family of three closely related proteins and functions as a GEF for Arf6 (Someya et al., 2001), the principal coat recruitment GTPase at the plasma membrane (D'Souza-Schorey and Chavrier, 2006). BRAG2-mediated Arf6 activation is required for myotube fusion (Chen et al., 2003; Pajcini et al., 2008) and regulates cell adhesion by triggering membrane trafficking events, including beta 1 integrin endocytosis (Dunphy et al., 2006). Moreover, BRAG2 is involved in the invasive activity of breast cancer cells by linking EGF receptor signaling to Arf6 activation (Morishige et al., 2008). A role for BRAG2 in the brain has not yet been described, although Arf6 has been implicated in the recruitment of AP2 and clathrin to synaptic membranes (Krauss et al., 2003). In cultured neurons, Arf6, activated by other Arf6-GEFs, ARNO, and EFA6A, controls the development of neurites and dendritic spines (Choi et al., 2006; Hernández-Deviez et al., 2002).

Notwithstanding the importance of LTD for cognitive functions and the detailed insight into various LTD induction pathways, the molecular events actually triggering AMPAR internalization for LTD have remained enigmatic. Here we show that AMPARs promote their own endocytosis for LTD through BRAG2-mediated Arf6 activation. We provide evidence that BRAG2 can

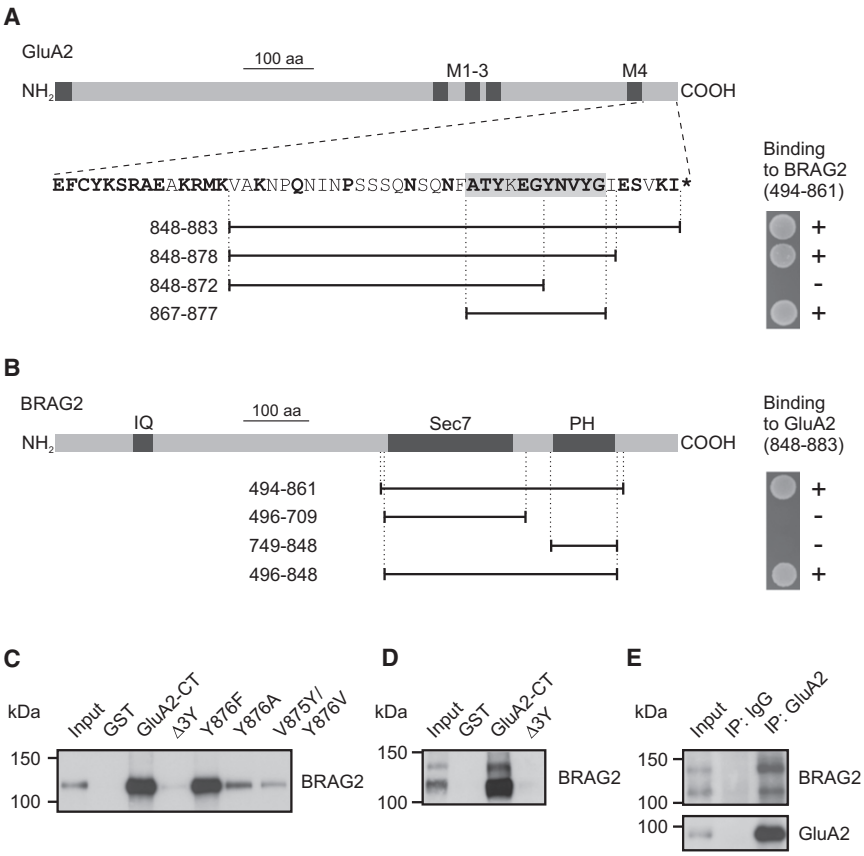

Figure 1. Protein-Protein Interaction between AMPARs and BRAG2

(A) A tyrosine-rich motif conserved between short-tailed AMPAR subunits mediates binding to BRAG2. Shown are C-terminal segments of rat GluA2 appended to the Gal4 DNA-binding domain. The ability of these fusion proteins to interact with a BRAG2 fragment (amino acids 494–861, encoded by a prey clone from the screen) in the Y2H assay is indicated on the right by the growth of cotransformed yeast colonies spotted on medium lacking histidine. An 11 amino acid motif with 3 tyrosine residues (3Y motif, shaded) was sufficient for binding to the BRAG2 prey. The single letter sequence of the C-terminal region of rat GluA2 highlights the amino acids conserved between GluA2, GluA3, and GluA4$_{short}$ (Gallo et al., 1992) in bold.

(B) The Sec7-PH module of BRAG2 interacts with the GluA2 C-terminal domain. The map of BRAG2 highlights the IQ motif, the Sec7 domain, and the PH domain. The prey protein and three deletion constructs with the specified amino acids of BRAG2 are aligned to the domain map. Their ability to interact with a C-terminal fragment of GluA2 (amino acids 848–883, the bait used for screening) in the Y2H assay is indicated on the right.

(C) Immunoblots of recombinant BRAG2 recovered by GST pull-down with GluA2-CT, Δ3Y (GluA2-CT lacking amino acids 867–877), Y876F, Y876A, or V875A/Y876V (GluA2-CT with the indicated amino acid changes) from HEK-BRAG2 cells. Input: 2.5%.

(D) Immunoblots of endogenous BRAG2 recovered by GST pull-down with GluA2-CT or Δ3Y from mouse forebrain extracts. Input: 2.5%.

(E) Immunoblots of endogenous BRAG2 coimmunoprecipitated (IP) by an antibody to GluA2 or control IgG from cultured hippocampal neurons. Input: 2%.

bind to synaptic AMPARs, is activated by the tyrosine-rich motif of GluA2, and is necessary for both mGluR- and NMDAR-dependent LTD (mGluR- and NMDAR-LTD) in CA1 cell synapses of the mouse hippocampus. Our results identify AMPAR-mediated Arf6 activation through BRAG2 as a critical mechanism for targeted synaptic receptor endocytosis that is dynamically regulated by both AMPAR ligand binding and the phosphorylation state of tyrosine 876 (Y876) in GluA2. This dual-key strategy provides tight control over the induction of LTD.

RESULTS

AMPARs Directly Interact with BRAG2

Using the C-terminal 36 amino acids of GluA2 as a bait in a yeast two-hybrid (Y2H) screen through a rat brain cDNA library, we found two overlapping cDNA clones encoding fragments of BRAG2 (Someya et al., 2001), a Sec7 domain protein functioning in membrane transport and remodeling (Dunphy et al., 2006; Morishige et al., 2008; Pajcini et al., 2008). Further Y2H analyses revealed that BRAG2 bound to all short AMPAR C-terminal regions (GluA2, GluA3, and GluA4$_{short}$), but not to the long C-terminal region of GluA1 (data not shown). Stepwise mutations of GluA2-CT indicated that the interaction did not require the extreme C terminus, but the tyrosine-rich motif (ATYKEGYNVY^{876}G, designated 3Y motif) implicated in LTD (Ahmadian et al., 2004) (Figure 1A). In BRAG2, only fragments encompassing the Sec7 and PH domains scored positive for binding to GluA2-CT (Figure 1B). The Sec7-PH regions of BRAG1, which shows the highest sequence similarity to BRAG2, or of ARNO, a more distantly related Arf6-GEF of the cytohesin/GRP1 family, did not bind to GluA2-CT in the Y2H system (data not shown). These data suggest that short-tailed AMPAR subunits specifically engage BRAG2 through their 3Y motif. Glutathione-S-transferase (GST) pull-down assays from lysates of HEK293 cells stably expressing rat BRAG2 or mouse forebrain extracts confirmed the physical interaction between BRAG2 and the 3Y motif of GluA2-CT, and coimmunoprecipitations indicated constitutive complex formation of GluA2 and BRAG2 in neurons (Figures 1C–1E; for specificity of the two immunoreactive BRAG2 bands, see Figure S3A available online). Moreover, these experiments revealed a critical role of Y876 in GluA2 for BRAG2 binding, as GluA2-CT mutants Y876A and V875Y/Y876V pulled down negligible amounts of BRAG2. However, BRAG2 binding was not affected by mutation Y876F in GluA2-CT.

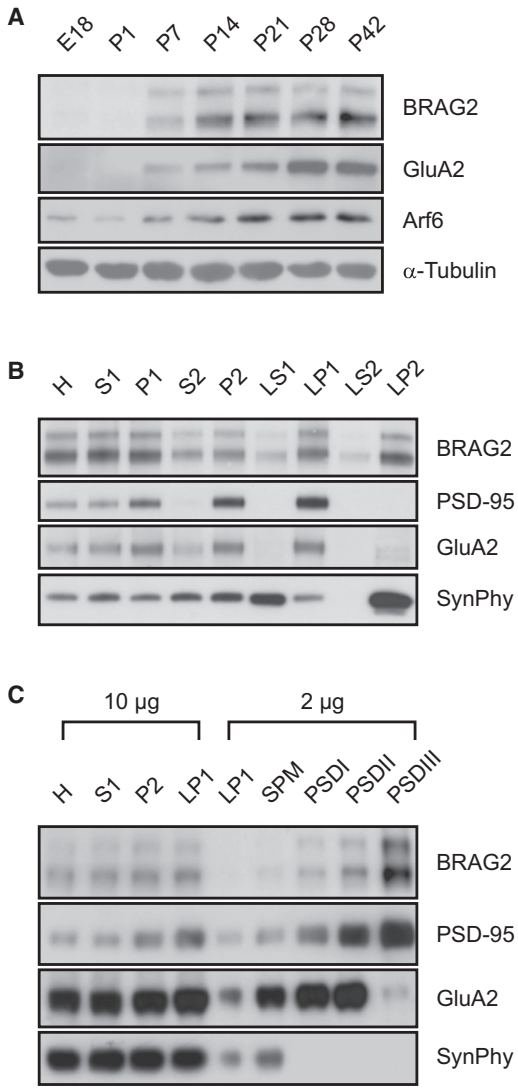

Figure 2. BRAG2 Is a Component of Mouse Brain Synapses

(A) Expression of BRAG2 in mouse hippocampus during development. E, embryonic day; P, postnatal day.

(B and C) Distribution of BRAG2 in mouse brain fractions revealing concentration in synaptic vesicle-enriched (B) and PSD fractions (C). H, homogenate; P1, crude nuclear fraction; S1, supernatant after P1 precipitation; P2, crude synaptosomal fraction; S2, supernatant after P2 precipitation; LP1, synaptosomal membranes (lysate pellet); LS1, crude synaptic vesicle fraction (lysate supernatant); LP2, synaptic vesicle-enriched fraction; LS2, synaptosomal cytosol; SPM, synaptosomal plasma membranes; PSD, postsynaptic density fraction extracted with Triton X-100 once (PSDI), twice (PSDII) or with Triton X-100 followed by N-lauroyl sarcosine (PSDIII); SynPhy, synaptophysin.

Thus, the phenyl ring of this tyrosine residue in GluA2 appears to be crucial for the interaction with BRAG2.

BRAG2 Is a Synaptic Protein

Expression of BRAG2 in the mouse hippocampus is very low at birth, but gradually increases, similar to GluA2 and Arf6, in parallel with synaptogenesis (Figure 2A). Upon differential centrifugation of adult mouse brain extracts, BRAG2 was detected in a fraction positive for the synaptic vesicle marker synaptophysin (Figure 2B); in addition, it is highly concentrated in postsynaptic density (PSD) fractions (Figure 2C), as suggested by previous mass spectrometry analyses (Jordan et al., 2004; Peng et al., 2004). Thus, the interaction between AMPARs and BRAG2 can take place at synapses. BRAG1 and BRAG3 are also enriched in PSD fractions (Inaba et al., 2004; Murphy et al., 2006), hinting at a role for the entire BRAG family of Arf6 exchange factors in synaptic membrane turnover.

AMPARs Directly Stimulate the Exchange Activity of BRAG2

BRAG2 encompasses an IQ motif, a Sec7, and a PH domain and functions as a GEF for the small GTPase Arf6 (Someya et al., 2001). Activation of Arf6 by the catalytic Sec7 domain results in the recruitment of vesicle coat proteins to the plasma membrane (D'Souza-Schorey and Chavrier, 2006), but the molecular mechanisms leading to GEF activation are poorly understood. The interaction between GluA2 and BRAG2 may provide a link between a receptor destined for internalization and the initiation of vesicle formation. Given that the Sec7-PH region of BRAG2 is involved in binding of GluA2 via GluA2-CT, we tested if this interaction might influence the activity of BRAG2 toward Arf6. Indeed, the bacterially expressed GluA2-CT increased the catalytic activity of BRAG2 on Arf6 about 5-fold in vitro (Figure 3A) but was without effect on the exchange rates of BRAG1 and ARNO (Figure 3B). Thus, the C terminus of GluA2 can trigger Arf6 activation through interaction with BRAG2.

Tyrosine Phosphorylation of GluA2 Controls BRAG2 Activity

The GluA2 3Y motif has been shown to be a target for a src family kinase-dependent phosphorylation in vivo, most likely at Y876 (Ahmadian et al., 2004; Hayashi and Huganir, 2004). Neither a V875Y/Y876V- nor a Y876A-mutated construct of GluA2-CT augmented the exchange rate of BRAG2, whereas a Y876F-mutated construct of GluA2-CT was fully active (Figure 3A), in accordance with the effects of these mutations on the BRAG2 interaction (Figure 1C). Using synthetic peptides encompassing the 3Y motif with either tyrosine or phosphotyrosine at position 876, we found that the unphosphorylated peptide increased the BRAG2 exchange rate, whereas the phosphorylated peptide did not (Figure 3C). Phosphatase treatment of the phosphorylated 3Y peptide restored the activity on BRAG2, demonstrating that the phosphorylation state of Y876 indeed determines the peptide's effect on the Arf6 exchange factor activity. We confirmed the regulatory effect of Y876 phosphorylation in the context of the complete intracellular C-terminal domain (Figure 3D): the increase in the catalytic activity of the BRAG2 Sec7 domain by GluA2-CT was blocked by prior in vitro phosphorylation with recombinant src kinase, whereas the increase mediated by the nonphosphorylatable Y876F mutant of GluA2-CT was not affected by src. An anti-phosphotyrosine antibody revealed that under these experimental conditions Y876 was the only amino acid residue targeted by src (Figure S1). Furthermore, we generated a site-specific phosphotyrosine antibody and detected src family kinase-dependent phosphorylation of Y876 in endogenous

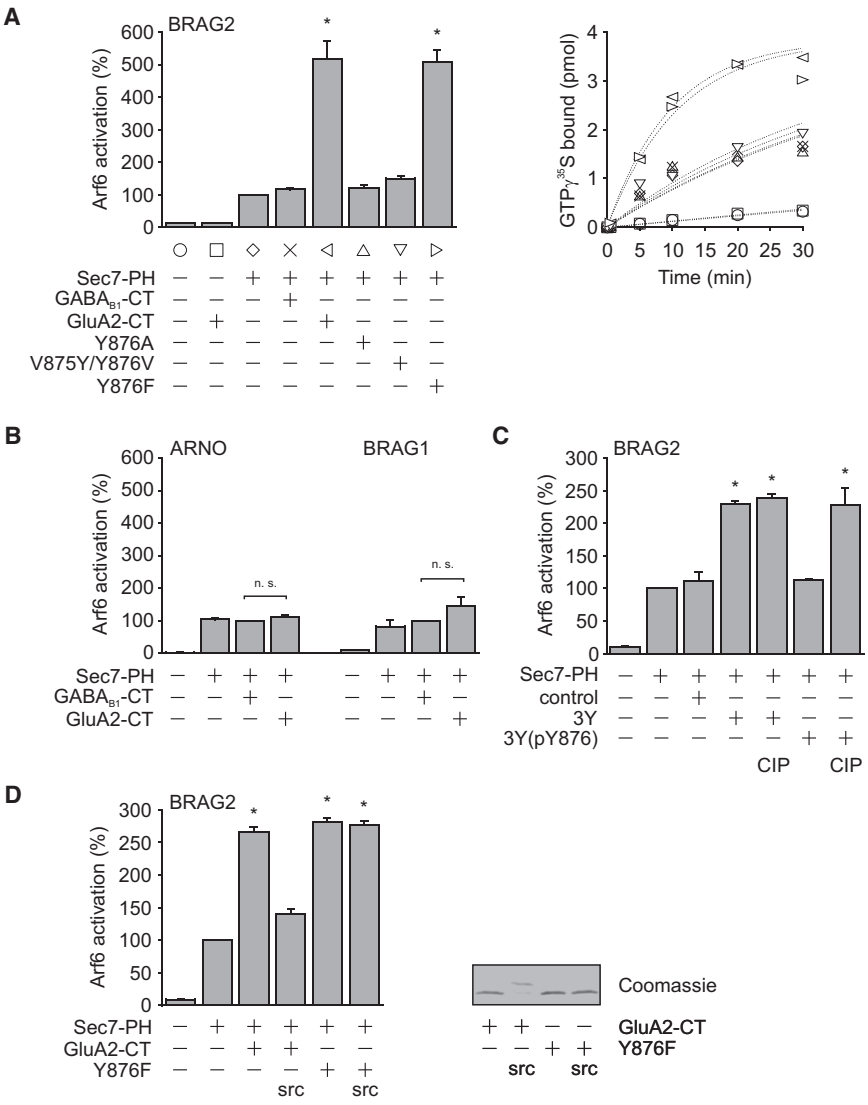

Figure 3. The C-Terminal Region of GluA2 Stimulates BRAG2-Mediated Arf6 Activation In Vitro

(A) GluA2-CT stimulates the GEF activity of BRAG2 depending on the integrity of the 3Y motif. Shown are the results of nucleotide exchange assays ($n \geq 3$) using the indicated purified proteins and Arf6-His in vitro. Bars indicate the initial reaction rate constants of GTPγ^{35}S binding (a representative experiment is indicated on the right) normalized to the combination Sec7-PH and Arf6-His (BRAG2, *$p \leq 0.0001$, $n = 7$). Sec7-PH, module of the Sec7 and PH domains of BRAG2; GABA$_{B1}$-CT, intracellular C-terminal region of GABA$_{B1}$; GluA2-CT variants as in Figure 1C.

(B) GluA2-CT does not stimulate the GEF activities of ARNO and BRAG1. Bars indicate the initial reaction rate constants of GTPγ^{35}S binding normalized to the combination Sec7-PH, Arf6-His, and GABA$_{B1}$-CT (ARNO, n. s., not significant: $p = 0.053$, $n = 8$; BRAG1, n. s.: $p = 0.15$, $n = 7$). Sec7-PH, modules of the Sec7 and PH domains of ARNO or BRAG1.

(C) Regulation of BRAG2-mediated Arf6 activation by 3Y peptides depends on the phosphorylation state of Y876. BRAG2 stimulation by synthetic peptides encompassing the tyrosine-rich motif of GluA2 (3Y) and a Y876-phosphorylated version thereof (pY876), with or without prior calf intestine phosphatase (CIP) treatment (*$p \leq 0.005$, $n = 4$). Control, unrelated peptide.

(D) Regulation of BRAG2-mediated Arf6 activation by GluA2-CT is blocked by phosphorylation of Y876. BRAG2 stimulation by GluA2-CT and the Y876F mutant, with or without prior phosphorylation by src (*$p \leq 0.0002$, $n = 6$). A phosphorylation-dependent change in the migration of GluA2-CT on SDS-PAGE was visualized by Coomassie staining.

All data are plotted as mean ± SEM. See also Figure S1.

GluA2 (Figure S2), suggesting in vivo relevance of this modification. Taken together, these data indicate that the phosphorylation state of GluA2 Y876 controls the BRAG2-mediated GDP/GTP exchange on Arf6.

AMPAR Ligand Binding Stimulates BRAG2

We subsequently assayed the Arf6 activity in a cellular environment. Brief stimulation of HEK293 cells coexpressing GluA2, BRAG2, and Arf6 with L-glutamate led to increased Arf6 activity, as assessed by an Arf6$_{GTP}$-specific pull-down assay (Santy and Casanova, 2001) (Figure 4A). This effect relied on BRAG2 expression and was prevented by the Y876A mutation in GluA2, which blocked Arf6 activation by GluA2-CT in vitro. Treatment with the partial AMPAR agonist CNQX, which is unable to open AMPA channels in absence of TARP auxiliary subunits (Menuz et al., 2007), also activated Arf6 in this setting (Figure 4B). Together, these findings confirm the functional connection between GluA2, BRAG2, and Arf6 and reveal ligand binding to GluA2 as a trigger of BRAG2 catalysis. Occupancy of the glutamate-binding site of AMPARs containing subunits with a 3Y motif can induce Arf6 activation by BRAG2, presumably independent of current flow.

Determinants Underlying Activation of Synaptic Arf6

Next, we monitored the activity of endogenous Arf6 in cultured hippocampal neurons. Our experiments with recombinant proteins suggested that both ligand binding and tyrosine phosphorylation may regulate Arf6 activation by AMPARs in concert. A 15 min treatment with picrotoxin to increase neuronal activity resulted in a slight increase in Arf6$_{GTP}$ (Figure 4C). Inhibition of src family tyrosine kinases by PP2, which prevented phosphorylation at Y876 of GluA2 (Figure S2C), activated neuronal Arf6 as well. However, a particularly strong Arf6 activation was observed upon combined treatment with PP2 and picrotoxin. Thus, neuronal Arf6 activity appears to be held in check by src family tyrosine kinases.

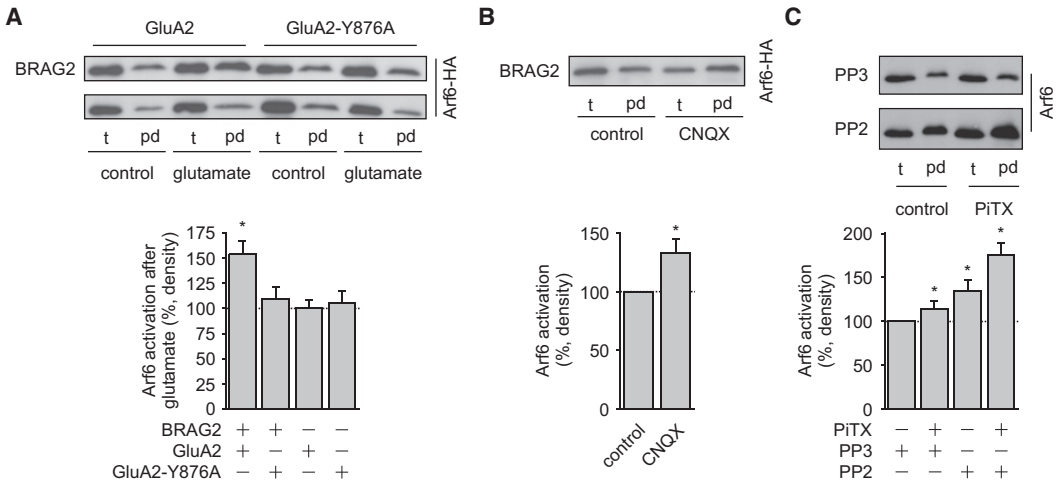

Figure 4. AMPAR Ligand Binding Stimulates BRAG2-Mediated Arf6 Activation

(A) L-glutamate-triggered BRAG2 stimulation. Shown are representative immunoblots of $Arf6_{GTP}$-specific pull-down assays ($n \geq 9$) from HEK293 and HEK-BRAG2 cells expressing Arf6-HA and either HA-tagged GluA2 or GluA2-Y876A. Bars illustrate Arf6 activation calculated as the $Arf6_{GTP}/Arf6_{total}$ ratio (pd/t) of cells treated with L-glutamate (*p = 0.001, n = 15) normalized to untreated controls.

(B) CNQX-triggered BRAG2 stimulation. Shown is a representative immunoblot of $Arf6_{GTP}$-specific pull-down assays (n = 10) from HEK-BRAG2 cells expressing Arf6-HA and HA-tagged GluA2. Bars illustrate Arf6 activation calculated as the $Arf6_{GTP}/Arf6_{total}$ ratio (pd/t) of cells treated with CNQX (*p = 0.01, n = 10) normalized to untreated controls.

(C) Activation of endogenous Arf6 is regulated by src family tyrosine kinases and neuronal activity. Shown are representative immunoblots of $Arf6_{GTP}$-specific pull-down assays from cultured hippocampal neurons pretreated with src family kinase inhibitor PP2 or its inactive structural analog PP3 and stimulated with picrotoxin (PiTX). The bar graphs illustrate Arf6 activation by PP3/PiTX (*p = 0.048), PP2 (*p = 0.006), and PP2/PiTX (*p = 0.00006) as the $Arf6_{GTP}/Arf6_{total}$ ratio (pd/t) normalized to PP3-treated controls (n = 15). pd, pull-down; t, total.

All data are plotted as mean ± SEM.

mGluR-Triggered Dephosphorylation of GluA2 Y876

The findings described so far are consistent with an important role of GluA2 Y876 phosphorylation in regulating synaptic Arf6 activity. A major form of Schaffer collateral LTD, mGluR-LTD, relies on tyrosine phosphatase activity and is accompanied by tyrosine dephosphorylation of GluA2 (Gladding et al., 2009; Huang and Hsu, 2006; Moult et al., 2006, 2008), but the exact tyrosine residue has not been determined. We therefore monitored mGluR-dependent changes in the phosphorylation level at Y876 in GluA2 using anti-pY876 (Figure S2) in neuronal cultures. An increase of the neuronal activity by picrotoxin, as frequently applied in mGluR-LTD experiments (Palmer et al., 1997), augmented phosphorylation of this site (Figure 5A), presumably through increased glutamate release and AMPAR ligand binding (Hayashi and Huganir, 2004; Hayashi et al., 1999). Importantly, additional application of DHPG, a selective agonist of group I mGluRs, strongly reduced pY876 (Figure 5B). These results directly show that phosphorylation of Y876, which was critical for BRAG2 stimulation in vitro (Figures 3C and 3D), dynamically responds to synaptic activity and mGluR engagement. Given the high sequence similarity between the 3Y motif of short-tailed AMPA receptor subunits (Figure 1A), we cannot completely rule out that GluA3 or $GluA4_{short}$ contribute to signals detected by anti-pY876, provided they are phosphorylated at the homologous residue. Nonetheless, our data identify Y876 as a residue in GluA2 targeted by a tyrosine phosphatase during mGluR-LTD.

BRAG2 Mediates mGluR-Induced Arf6 Activation

We went on analyzing the nucleotide-binding state of Arf6 following mGluR activation. Short treatment with DHPG triggered an increase in the amount of active Arf6, reminiscent of the PP2 effect (Figures 5C and 4C). Combined application revealed that the effects of DHPG and PP2 were not additive, but occlusive. The two independent tyrosine phosphatase inhibitors sodium orthovanadate (OV) and phenylarsine oxide (PAO), which prevent mGluR-LTD (Moult et al., 2006), blocked the DHPG effect without affecting basal Arf6 activation, indicating that tyrosine dephosphorylation is necessary for DHPG-induced Arf6 activation in cultured neurons. In conjunction with our findings with recombinant proteins (Figure 3) and our analysis employing anti-pY876 (Figure 5B), the above data are consistent with the hypothesis that DHPG-triggered Arf6 activation is mediated by dephosphorylation of Y876 in GluA2 and subsequent BRAG2 stimulation. Indeed, suppression of BRAG2 expression by RNA interference (RNAi) with lentivirally delivered short-hairpin RNAs (Figure S3A) prevented the DHPG effect (Figure 5D). Therefore, BRAG2 is required for Arf6 activation following DHPG stimulation.

BRAG2-Mediated Arf6 Activation Is an Essential Step in mGluR-Induced AMPAR Internalization

Expression of mGluR-LTD, like several other forms of LTD, relies on regulated endocytosis, resulting in a persistent decrease of surface AMPARs. Since Arf6 is a well-known regulator of endocytic transport at the cell surface, we assessed whether BRAG2

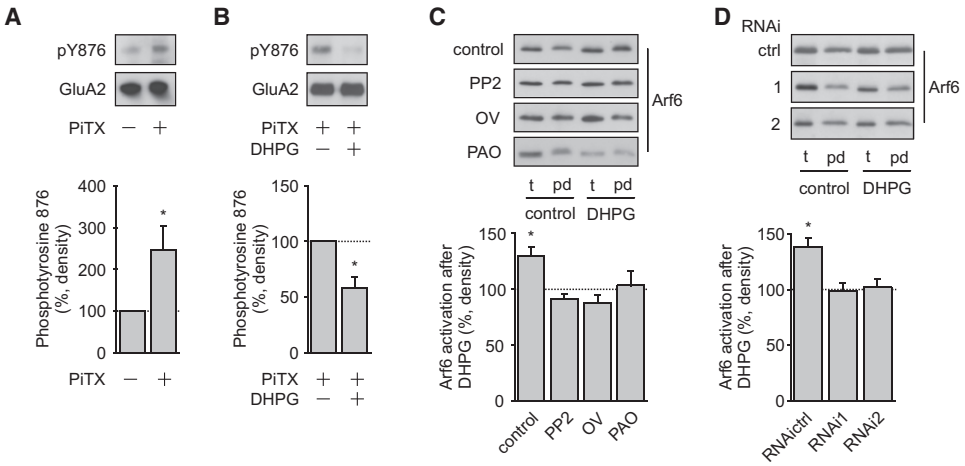

Figure 5. mGluRs Trigger Dephosphorylation of GluA2 Y876 and BRAG2-Mediated Arf6 Activation

(A) Phosphorylation of GluA2 Y876 in cultured hippocampal neurons upon picrotoxin (PiTX) treatment. The bars show pY876/GluA2-ratios of GluA2 immunoprecipitates from neurons treated with PiTX normalized to unstimulated controls (*p = 0.033, n = 5), Top: representative immunoblot.

(B) Dephosphorylation of GluA2 Y876 upon DHPG treatment. The bars show pY876/GluA2 ratios of GluA2 immunoprecipitates from neurons treated with PiTX/DHPG normalized to PiTX-treated controls (*p = 0.007, n = 5). Top: representative immunoblot.

(C) DHPG stimulates Arf6 activation in cultured neurons depending on tyrosine phosphatase activity. Shown are results of $Arf6_{GTP}$-specific pull-down assays from 3- to 4-week-old cultured hippocampal neurons, pretreated or not with the src family kinase inhibitor PP2 or tyrosine phosphatase inhibitors (OV, PAO), and stimulated with DHPG. Arf6 activation by DHPG was calculated as the $Arf6_{GTP}/Arf6_{total}$ ratio (pd/t) normalized to the respective control without DHPG (*p = 0.008, n = 6). Basal Arf6 activation was selectively increased by PP2 (123% ± 8% of control, p = 0.02, n = 5). Top: representative immunoblots. pd, pull-down; t, total.

(D) DHPG-stimulated Arf6 activation is prevented by RNAi to BRAG2. Cultured hippocampal neurons infected with lentiviruses delivering RNAi to BRAG2 (RNAi1, RNAi2) or a control hairpin (RNAictrl) were treated with or without DHPG. The bar graphs illustrate DHPG-stimulated Arf6 activation calculated as in (C) (*p = 0.0008, n = 9). Top: representative immunoblots.

All data are plotted as mean ± SEM. See also Figures S2 and S3.

also played a role in the sustained decrease of surface AMPARs after DHPG treatment of neurons (Snyder et al., 2001). Two independent assays for monitoring the surface expression of GluA2 yielded the same result: the reduction of surface-expressed GluA2 by DHPG was prevented by knockdown of BRAG2 (Figures 6A and 6B). We conclude that BRAG2 is not only essential for Arf6 activation, but also for the long-term reduction of surface AMPARs induced via mGluRs. Expression of a catalytically inactive form of BRAG2 (Figures S3B and S3C) or of an Arf6 mutant incapable of GTP binding (Macia et al., 2004) blocked the DHPG-induced reduction of surface GluA2 as well, confirming the critical role of BRAG2-mediated Arf6 activation in this signal transduction pathway (Figures 6C and 6D). Moreover, the surface reduction of GluA2 upon DHPG treatment was prevented by the competitive AMPAR antagonist NBQX (Figure 6E), indicating a requirement for agonist-dependent AMPAR signaling to BRAG2 (Figure 4A and 4B). An increased rate of endocytosis contributes to the persistent reduction of surface AMPARs induced by mGluRs (Gladding et al., 2009; Waung et al., 2008). We therefore directly assessed the mGluR-induced GluA2 internalization and found that it strictly depends on the catalytic activity of BRAG2 (Figure 6F). None of the manipulations of BRAG2, neither knockdown nor expression of recombinant BRAG2 constructs, affected the basal amount of surface GluA2 (Figure S3D). Together, BRAG2 appears to translate ligand binding and tyrosine dephosphorylation of GluA2 into Arf6 activation for mGluR-controlled endocytosis of AMPARs.

mGluR-LTD in Hippocampal CA1 Neurons Depends on BRAG2

We next applied lentiviral BRAG2-RNAi to the hippocampal CA1 region by stereotaxic injection in 3-week-old mice and assessed mGluR-LTD in acute hippocampal slices 2 weeks after viral infection. Excitatory postsynaptic currents (EPSCs) in RNAi-infected, mock-infected, and noninfected CA1 pyramidal neurons were comparable before DHPG perfusion. DHPG strongly depressed EPSCs within 10 min by about 70% in all three groups (Figure 7A). During DHPG washout, neurons from mock-infected and noninfected neurons partially recovered to about 60% of control, and LTD became apparent in both groups. In contrast, EPSCs in RNAi-infected neurons steadily recovered, reaching baseline 40 min after terminating DHPG perfusion. 30 min after terminating DHPG perfusion, RNAi-infected neurons (87.3% ± 4.3%, n = 11 neurons, 9 mice) significantly differed from mock-infected (57.5% ± 6.8%, n = 7 neurons, 4 mice; p = 0.002) and noninfected neurons (60.5% ± 5.0%, n = 9 neurons, 7 mice; p = 0.0004). Thus, knockdown of BRAG2 prevented the expression of LTD but did not interfere with the initial DHPG effects, which also occur in the presence of endocytosis inhibitors (Xiao et al., 2001).

In addition, we generated mice in which loxP sites flank the essential exon 2 of the BRAG2 gene *Iqsec1* (*Iqsec1*$^{fl/fl}$), thus permitting Cre-mediated deletion of the gene (Figures S4A and S4C). BRAG2 expression did not differ between wild-type and *Iqsec1*$^{fl/fl}$ mice (Figure S4B). We injected a lentiviral vector expressing Cre recombinase and EGFP into the hippocampal CA1 region of

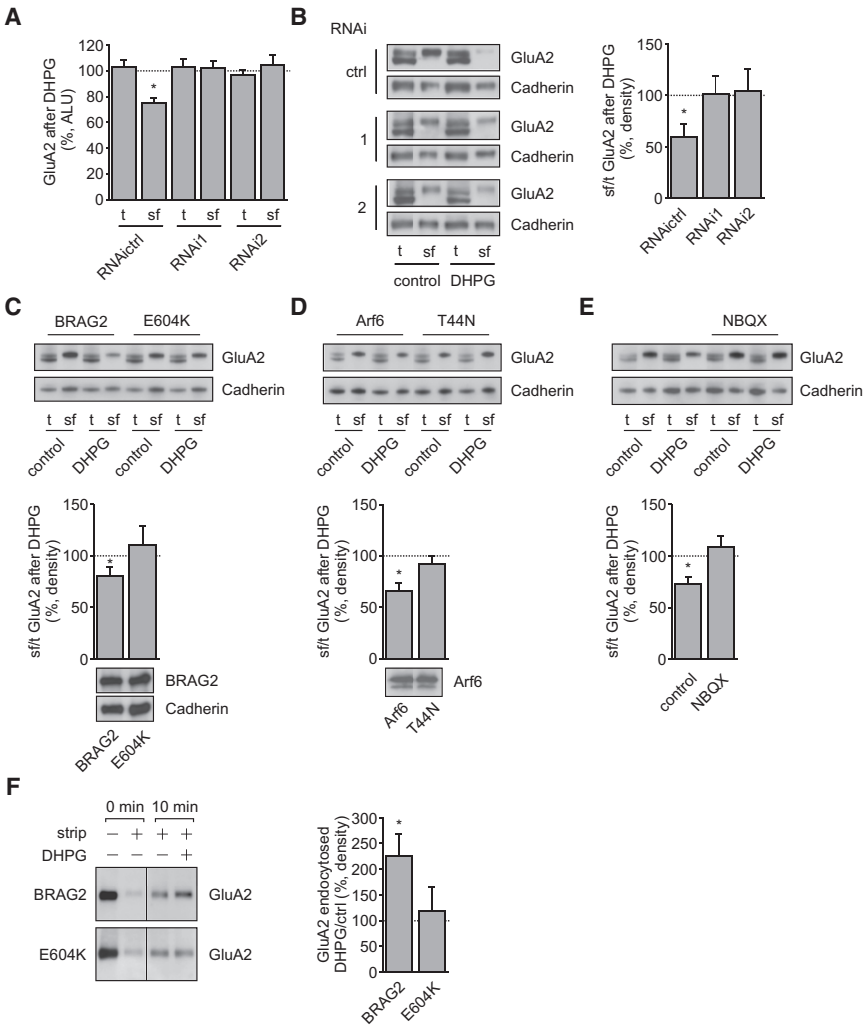

Figure 6. AMPAR-BRAG2 Signaling to Arf6 Is Necessary for mGluR-Induced Internalization of AMPARs

(A) DHPG-triggered long-term reduction of surface GluA2 is mediated by BRAG2. Cultured hippocampal neurons infected with lentiviruses delivering RNAi to BRAG2 as described in Figure 5D were treated with or without DHPG and analyzed for both total and surface GluA2 expression using a cell ELISA. The bars depict the GluA2 total (t) and surface (sf) expression of neurons 55 min after terminating DHPG treatment (5 min) normalized to the respective untreated controls ($n \geq 6$). DHPG treatment resulted in a selective reduction of surface GluA2 (*$p = 0.00003$, $n = 12$), and this effect was blocked by RNAi to BRAG2 (RNAi1, $p = 0.31$, $n = 6$; RNAi2, $p = 0.28$, $n = 6$). ALU, arbitrary light units.

(B) Neurons were infected and stimulated as in (A), but total and surface levels of endogenous GluA2 were quantified using a surface biotinylation assay. The bars depict the GluA2 surface/total ratios (sf/t) of neurons 1 hr after treatment with DHPG normalized to the respective untreated controls. DHPG treatment resulted in a selective reduction of the GluA2 surface expression (*$p = 0.005$, $n = 8$), and this effect was blocked by RNAi to BRAG2 (RNAi1, $p = 0.48$, $n = 8$; RNAi2, $p = 0.41$, $n = 8$). Representative immunoblots to GluA2 and Cadherin are shown on the left.

(C) DHPG-triggered long-term removal of surface GluA2 relies on the catalytic activity of BRAG2. Neurons infected with lentiviruses for expression of BRAG2-EGFP (BRAG2) or a catalytically inactive mutant (E604K) were stimulated and analyzed as in (B). DHPG treatment resulted in a selective reduction of GluA2 surface levels in neurons expressing BRAG2 (*$p = 0.034$, $n = 9$), and this effect was blocked upon expression of the E604K mutant ($p = 0.28$, $n = 13$). Representative immunoblots to GluA2 and Cadherin are shown on top. A comparison between the expression of BRAG2 and E604K is shown beneath the bar graphs.

(D) DHPG-triggered long-term removal of surface GluA2 requires active Arf6. Neurons infected with lentiviruses for expression of Arf6-HA (Arf6) or a constitutively inactive mutant (T44N) were treated and analyzed as in (B). DHPG treatment resulted in a selective reduction of GluA2 surface expression in neurons expressing Arf6 (*$p = 0.002$, $n = 5$), and this effect was blocked by expression of Arf6-T44N ($p = 0.46$, $n = 5$). Representative immunoblots to GluA2 and Cadherin are shown on top. Expression of HA-tagged Arf6 and Arf6-T44N as compared to endogenous Arf6 (lower bands) is shown beneath the bar graphs.

(E) AMPA receptor ligand binding is necessary for DHPG-triggered long-term removal of surface GluA2. Uninfected neurons were stimulated with DHPG for 5 min and incubated for 55 min, in absence or sustained presence of the AMPA receptor antagonist NBQX. Surface and total amounts of GluA2 and Cadherin were analyzed as in (B). DHPG treatment resulted in a selective reduction of GluA2 surface expression in absence of NBQX (*$p = 0.001$, $n = 9$), and this effect was blocked by NBQX ($p = 0.24$, $n = 9$). Representative immunoblots to GluA2 and Cadherin are shown on top.

(F) BRAG2-mediated Arf6 activation is necessary for DHPG-induced endocytosis of GluA2. Neurons infected as in (C) were analyzed for DHPG-triggered endocytosis of GluA2 using reversible surface biotinylation. The bars depict the amount of GluA2 internalized within 10 min upon DHPG treatment as the percentage of basal internalization. Background levels of GluA2 without internalization (0 min) were subtracted from all values. Internalization of GluA2 was significantly increased in DHPG-treated cultures expressing BRAG2 (*$p = 0.01$, $n = 9$), and this effect was blocked upon expression of catalytically inactive mutant E604K ($p = 0.34$, $n = 9$). Strip, removal of biotin from the cell surface.

All data are plotted as mean ± SEM. See also Figure S3.

3-week-old *Iqsec1*$^{fl/fl}$ mice and investigated mGluR-LTD 2 weeks later (Figure 7B). The DHPG response of CA1 neurons having undergone Cre-mediated deletion of BRAG2 was similar to the response recorded after RNAi-mediated knockdown of BRAG2. In the absence of BRAG2, the currents recovered to baseline within 30 min after DHPG perfusion (101.2% ± 5.1%, n = 8 neurons, 5 mice), whereas LTD was induced in noninfected neurons (60.8% ± 4.4%, n = 7 neurons, 5 mice; $p = 0.00002$ between groups). Collectively, our results clearly show that BRAG2 is essential for hippocampal mGluR-LTD.

BRAG2 Binding to GluA2 Is Necessary for mGluR-LTD

To examine whether the interaction of BRAG2 with GluA2 is critical for mGluR-LTD, we employed peptide competition. Peptides

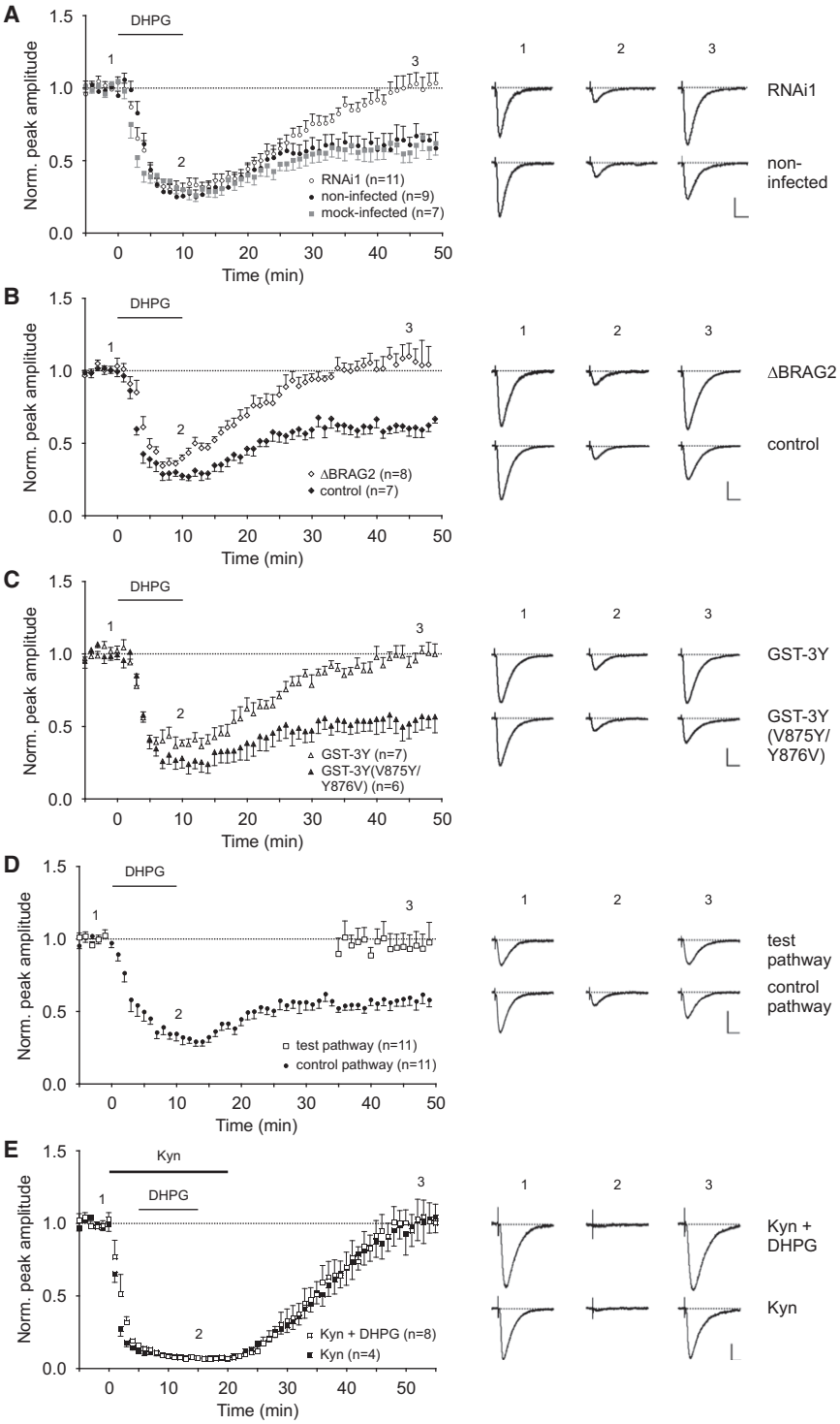

Figure 7. BRAG2 and AMPAR Ligand Binding Are Necessary for mGluR-LTD of Schaffer Collateral Synapses

(A) Cell-specific knockdown of BRAG2 blocks mGluR-LTD at hippocampal CA3-CA1 synapses. Acute slices of in vivo-infected mice (surgery at P21; electrophysiology 2 weeks later) were treated with DHPG, which induced mGluR-LTD in control CA1 neurons (noninfected or mock-infected), but not in neurons infected with lentiviruses delivering shRNAs against BRAG2 (RNAi).

(B) Deletion of BRAG2 in single CA1 neurons blocks mGluR-LTD. Experiments performed as described in (A), except that Cre-expressing lentiviruses were injected into mice homozygous for a floxed BRAG2 allele (*Iqsec1*$^{fl/fl}$). Results for cre-infected (ΔBRAG2) and noninfected (control) neurons are shown.

(C) Acute blockade of the interaction between GluA2 and BRAG2 prevents mGluR-LTD. Shown are mGluR-LTD analyses in hippocampal slices of wild-type mice with a recombinant GST fusion protein containing the 3Y sequence YKEGYNVYGI (GST-3Y), or a control with a single amino acid permutation, reading YKEGYNYVGI [GST-3Y(V875Y/Y876V)], back-filled into the patch pipette at 100 μg/ml prior to DHPG perfusion.

(D and E) mGluR-LTD requires AMPAR ligand binding. CA1 neurons in hippocampal slices of wild-type mice were stimulated by two independent pathways (test and control pathway). Interruption of stimulation in the test pathway during and following DHPG perfusion (35 min) prevented mGluR-LTD induction (D). Presence of the broad-spectrum ionotropic glutamate receptor antagonist kynurenic acid (Kyn) prevented mGluR-LTD induction by DHPG in wild-type mice (E).

(A–E) Six consecutive traces were averaged at time points marked by numbers in the respective time course. Scale bars: 50 pA, 20 ms. All data points are plotted as mean ± SEM. See also Figures S3 and S4.

with the 3Y motif of GluA2 interfere with LTD induced by different protocols (Ahmadian et al., 2004; Brebner et al., 2005; Fox et al., 2007; Yu et al., 2008), but mGluR-LTD has not been assessed. We found that inclusion of the active 3Y peptide fused to GST (GST-3Y) in the patch pipette blocked mGluR-LTD expression in CA1 neurons from 5-week-old wild-type mice with the same time course as observed in neurons infected with either BRAG2-RNAi in wild-type or with Cre in *Iqsec1*$^{fl/fl}$ mice (Figure 7C). In contrast, GST fused to a 3Y peptide with the V875Y/Y876V permutation [GST-3Y(V875Y/Y876V)] that abrogates binding to BRAG2 (Figure 1C) remained inactive. 30 min after terminating DHPG perfusion, GST-3Y-infused neurons (88.31% ± 4.2%, n = 7 neurons, 5 mice) were significantly different from GST-3Y(V875Y/Y876V)-infused neurons (53.0% ± 7.2%, n = 6 neurons, 4 mice; p = 0.001). These experiments indicate that the relevant effect of the active 3Y peptide is interference with BRAG2 binding. The match between the results of chronic BRAG2 ablation and acute peptide competition further corroborates the functional link between the 3Y motif of GluA2 and BRAG2.

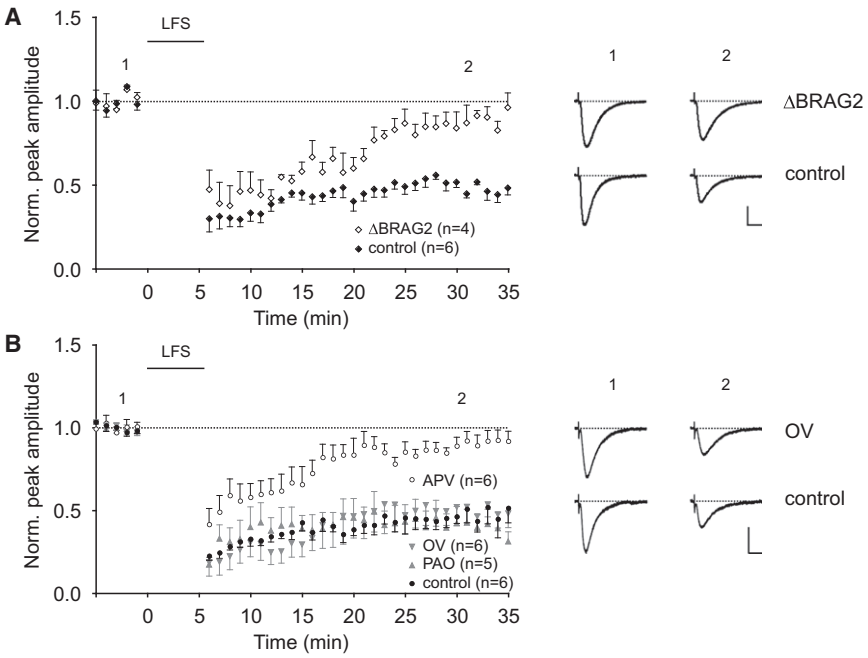

Figure 8. NMDAR-LTD Is Mediated by BRAG2

(A) Deletion of BRAG2 in single CA1 neurons blocks NMDAR-LTD. Low-frequency (2.5 Hz) stimulation of Schaffer collaterals for 6 min in presence of mGluR antagonists BAY 36-7620 and MPEP-HCl induced LTD in noninfected (control) but not in Cre virus-infected (ΔBRAG2) CA1 neurons of P35 *Iqsec1*$^{fl/fl}$ mice.

(B) NMDAR-LTD is independent of tyrosine dephosphorylation. NMDAR-LTD (control) was not altered in the presence of tyrosine phosphatase inhibitors (PAO, OV) but was inhibited in the presence of an NMDA receptor antagonist (APV) in CA1 neurons of wild-type mice.

(A and B) For details regarding traces, scale bars, and data points, see Figure 7.

See also Figure S4.

AMPAR Ligand Binding Is Necessary for mGluR-LTD

Experiments in HEK293 cells showed increased BRAG2-dependent Arf6 activation in the presence of AMPAR ligands (Figures 4A and 4B) and the competitive AMPAR antagonist NBQX blocked the DHPG-induced persistent reduction of surface AMPARs in dissociated neurons (Figure 6E). To test whether glutamate binding to AMPARs is necessary for mGluR-LTD in the hippocampus, we stimulated two independent pathways in stratum radiatum before DHPG perfusion. Stimulation was stopped in one pathway during and 25 min following DHPG perfusion and then resumed for 15 min, whereas stimulation proceeded in the second pathway. If ligand binding to AMPARs is necessary for mGluR-LTD, interruption of stimulation should prevent its expression. Indeed, mGluR-LTD was not induced in the pathway with interrupted stimulation, whereas mGluR-LTD was induced in the second pathway (Figure 7D). Compared to baseline, EPSCs were only reduced in the stimulated pathway 35 min after terminating DHPG perfusion (58.9% ± 5.2%, p = 0.005 versus 94.7% ± 9.5%, p = 0.3; n = 11 neurons, 5 mice). To corroborate this finding, we activated mGluRs while ionotropic glutamate receptors were antagonized by kynurenic acid (Kyn, 2 mM) (Figure 7E). Following washout of Kyn, EPSCs recovered to baseline within 30 min, indicating that DHPG did not induce LTD under these conditions (101.5% ± 8.6%, p = 0.4; n = 8 neurons, 4 mice). EPSCs similarly (p = 0.4) recovered when Kyn was perfused alone (98.9% ± 13.3%, p = 0.4; n = 4 neurons, 3 mice). These results substantiate a critical role for AMPAR ligand binding in mGluR-LTD.

Both mGluR- and NMDAR-LTD Rely on BRAG2

So far, our data revealed the importance of the interaction between the 3Y motif in GluA2 and BRAG2 for mGluR-LTD. However, the effect of 3Y peptides on LTD induced through different pathways indicates a general requirement of interactions mediated by this motif for LTD expression. We therefore asked if BRAG2 was also involved in NMDAR-LTD using the cell-specific Cre-mediated BRAG2 deletion strategy described above (Figure 8A). Low-frequency stimulation (LFS) of the Schaffer collaterals in the presence of mGluR antagonists induced LTD in noninfected (46.7% ± 2.5%, n = 5 neurons, 3 mice) but not Cre-infected neurons of *Iqsec1*$^{fl/fl}$ mice (91.1% ± 4.6%, n = 4 neurons, 3 mice; p = 0.0002 between groups). This LFS-induced LTD (LFS-LTD) was blocked by the NMDAR antagonist D-APV (50 μM) (Figure 8B; 90.9% ± 5.1%, n = 6 neurons, 4 mice; p = 0.3 compared to baseline). Thus, expression of BRAG2 in CA1 neurons is necessary for both mGluR- and NMDAR-LTD of Schaffer collateral projections. Chemically induced NMDAR-LTD was shown to be independent of tyrosine dephosphorylation (Moult et al., 2006). In accord, the tyrosine phosphatase inhibitor OV (1 mM) or PAO (15 μM) did not affect NMDAR-LTD induced by LFS (control: 48.1% ± 6.7%, n = 6 neurons, 5 mice; OV: 49.7% ± 8.4%, n = 6 neurons, 3 mice, p = 0.4; PAO: 38.8% ± 7.8%, n = 5 neurons, 3 mice, p = 0.2). We conclude that diverse pathways stimulating clathrin-mediated AMPAR endocytosis converge on GluA2-associated BRAG2.

DISCUSSION

LTD is a modification in synaptic strength involved in learning events in various brain areas (Massey and Bashir, 2007). Here we show that the Arf6-GEF BRAG2 is essential for hippocampal LTD. Depending on the phosphorylation state of Y876 in GluA2, BRAG2 translates AMPAR ligand binding into Arf6 activation, which in turn triggers AMPAR internalization for persistent synaptic depression. Thus, AMPARs control their own removal from the synapse through BRAG2.

As holds true for the other two members of the BRAG family (Inaba et al., 2004; Murphy et al., 2006), we found BRAG2 to be concentrated in PSD fractions and to resist detergent extraction, indicative of core elements of this postsynaptic

specialization. Therefore, it seems likely that BRAG2 binds and affects primarily synaptic AMPARs. GluA2 and BRAG2 could be coimmunoprecipitated from cultured neurons independent of LTD-inducing stimuli, suggesting that a significant fraction of AMPARs interacts constitutively with BRAG2.

GEF Activity of BRAG2 Controlled by Protein-Protein Interaction

The binding of the tyrosine-rich sequence motif of AMPARs to the Sec7-PH module of BRAG2 resulted in a strong augmentation of the catalytic activity of BRAG2. This is a surprising new feature in Arf-GEF regulation, given that in the closely examined Arf6-GEFs of the cytohesin/Grp1 family, which also contain a Sec7-PH tandem, binding of specific phosphatidylinositol phosphate species to the PH domain enhances the exchange activity of the catalytic Sec7 domain (Chardin et al., 1996; Klarlund et al., 1997). In stark contrast, the catalytic activity of BRAG2 is unaffected by phospholipids, and the PH domain of BRAG2 shows a low degree of conservation compared to the one of cytohesins, which suggested distinct binding partners of these two Arf6-GEF families (Someya et al., 2001). Recently, the PH domain of BRAG2 was shown to interact with the phosphorylated C terminus of the EGF receptor (Morishige et al., 2008). Together with our data, this suggests that the PH domain of BRAG2 may have evolved to sense intracellular domains of surface receptors instead of plasma membrane lipid modifications for regulation of the Sec7 activity. Based on their conservation, the PH domains of the other BRAG family members are likely to mediate a similar function for different membrane proteins.

Determinants of AMPAR-Associated BRAG2 Activity

Our data reveal that the activation of BRAG2 by AMPARs is tightly regulated. We provide evidence that ligand binding to GluA2 in heterologous cells stimulates BRAG2 and that an increase in the synaptic activity of neuronal cultures leads to Arf6 activation, particularly if tyrosine phosphorylation is pharmacologically inhibited. These data indicate that ligand binding to unphosphorylated AMPARs can trigger BRAG2 catalysis. Consistently, mGluR-LTD in hippocampal slices required not only BRAG2 but also persistent synaptic activity. The latter requirement was not found for mGluR-LTD induced under experimental conditions allowing postsynaptic depolarizations and/or involving presynaptic expression mechanisms (Fitzjohn et al., 2001; Huber et al., 2001). However, we confirmed that AMPAR activation is crucial, since both induction of mGluR-LTD in slices and DHPG-induced reduction in surface GluA2 in neuronal cultures were prevented by application of ionotropic glutamate receptor antagonists. Thus, we conclude that AMPAR ligand binding triggers, besides channel opening, signal transduction through the intracellular C-terminal region regulating endocytic traffic. The details of how occupancy of the glutamate-binding site translates into conformational changes at the C-tail of GluA2 for BRAG2 activation remain to be determined.

In addition, BRAG2 stimulation is controlled by phosphorylation of Y876 in GluA2. Our data reveal that phosphorylation of this tyrosine residue interferes with the signal transduction from GluA2 to BRAG2. Glutamate receptor agonist treatment causes tyrosine phosphorylation of GluA2 (Hayashi and Huganir, 2004), and we show that increased synaptic activity actually induces phosphorylation of GluA2 Y876. Thus, it appears that AMPAR-BRAG2 signaling is precluded during basal synaptic transmission by phosphorylation at Y876 in GluA2. Interestingly, a mutant of GluA2 that cannot be phosphorylated at the relevant position (Y876F) showed reduced clustering, surface expression, and synaptic localization as compared to the wild-type subunit (Hayashi and Huganir, 2004). Hence, phosphorylation of GluA2 Y876 may stabilize AMPARs at active synapses by protecting AMPARs from ligand-induced BRAG2 stimulation and internalization.

A series of conclusive experiments established that a tyrosine phosphatase activity is necessary for induction of mGluR-LTD (Huang and Hsu, 2006; Moult et al., 2006, 2008) and that tyrosine dephosphorylation of GluA2 occurs transiently at cell surface AMPARs during mGluR-LTD (Gladding et al., 2009; Huang and Hsu, 2006; Moult et al., 2006). Our data reveal that the combination of AMPAR ligand binding and dephosphorylation of GluA2 Y876 triggers BRAG2-mediated Arf6 activation during mGluR-LTD. Thus, a dual key strategy ensures that ligand-engaged AMPARs enter into the endocytic route only during LTD.

A Converging Step in mGluR- and NMDAR-LTD

We found that BRAG2 is required at hippocampal synapses not only for mGluR-LTD but also for NMDAR-LTD, which differ considerably in their molecular mechanisms and do not occlude each other (Nicoll et al., 1998; Oliet et al., 1997). This result indicates that the GluA2-BRAG2 interaction constitutes a crucial requirement for regulated synaptic depression in general, considering that the previously published effects of the GluA2 3Y peptides on LTD (Ahmadian et al., 2004; Brebner et al., 2005; Fox et al., 2007; Van den Oever et al., 2008; Yu et al., 2008) rely on competition with BRAG2 binding. It is therefore tempting to speculate that NMDAR-LTD also requires BRAG2 stimulation triggered by AMPARs with GluA2 Y876 in the unphosphorylated state. However, while NMDAR-LTD has been shown to rely on dephosphorylation of serine 845 in GluA1 (Lee et al., 2003, 2010), unlike mGluR-LTD it does not require acute tyrosine dephosphorylation (Moult et al., 2006) (Figure 8B). It remains to be resolved how GluA2-associated BRAG2 is activated independently of tyrosine phosphatase activity. The simplest scenario may be that NMDAR-LTD compromises ligand-binding-dependent phosphorylation of Y876 in GluA2, although NMDA treatment of hippocampal slices did not significantly reduce the overall AMPAR tyrosine phosphorylation state (Gladding et al., 2009). Alternatively, during NMDAR-LTD, BRAG2 activity may be regulated through Ca^{2+}/calmodulin interactions with the IQ motif (but see Someya et al. [2001]) or through serine/threonine phosphorylation of BRAG2 (Munton et al., 2007).

LFS induced NMDAR-LTD in Schaffer collaterals of young GluA2A3 knockout mice (Meng et al., 2003), and cultured hippocampal neurons derived from these mice showed NMDA-dependent, clathrin-mediated AMPAR endocytosis (Biou et al., 2008). These data clearly show that regulated AMPAR endocytosis can occur independently of the AMPAR-BRAG2 link. However, in the light of the large body of evidence supporting the role of

GluA2 in LTD (Kessels and Malinow, 2009; Malenka and Bear, 2004; Shepherd and Huganir, 2007), the targeted deletion of GluA2A3 most likely resulted in a modified LTD mechanism that is normally not expressed in CA1 neurons. The synaptic targeting of homomeric GluA1 receptors, which mediate the EPSCs in CA1 neurons lacking GluA2 and GluA3, is severely compromised (Lu et al., 2009). The altered subunit composition has consequences for the equilibrium between synaptic and extrasynaptic AMPARs and may also affect their lateral membrane diffusion and endocytic traffic. Indeed, LTD was less sensitive to blockade of endocytosis in GluA2A3 knockout than in wild-type mice (Meng et al., 2003). In mature wild-type CA1 neurons, all synaptic AMPARs contain the GluA2 subunit (Lu et al., 2009), allowing AMPAR endocytosis for NMDAR- and mGluR-LTD to be controlled by the interaction between GluA2 and BRAG2.

Role of Arf6 in LTD

Our data identify BRAG2-mediated Arf6 activation as a critical step in DHPG-induced AMPAR endocytosis and in LTD, raising the question of the direct function of activated Arf6 at the synapse. Arf6 plays a role in actin and membrane remodeling (D'Souza-Schorey and Chavrier, 2006), processes that are intimately involved in the modulation of excitatory synapses. The localized activation of Arf6 may trigger changes in the actin cytoskeleton, which not only are crucial for regulated AMPAR trafficking but also underlie morphological plasticity of dendritic spines (Derkach et al., 2007). In fact, BRAG2-mediated Arf6 activation has been shown to be important for structural changes of cell-to-cell contact sites, mediating processes of myotube fusion and cancer invasion (Morishige et al., 2008; Pajcini et al., 2008), and Arf6 is involved in the development of dendritic spines (Choi et al., 2006). It is therefore conceivable that upon LTD induction the AMPAR-induced Arf6 activation through BRAG2 links the reduction in surface receptor levels to changes in spine morphology, thus balancing efficacy and structure of the postsynaptic specialization.

Importantly, however, Arf6 activation also contributes directly to the formation of clathrin-coated vesicles at the plasma membrane. It does so by triggering a local increase in phosphatidylinositol (4,5)-bisphosphate [PtdIns(4,5)P_2], which mediates the initial contact of the clathrin adaptor complex AP2 with the plasma membrane (Krauss et al., 2003), and by direct interaction of AP2 with GTP-bound Arf6 (Paleotti et al., 2005). Moreover, AP2 can directly bind to GluA2-CT (Kastning et al., 2007; Lee et al., 2002), and a combination of PtdIns(4,5)P_2 and of binding sites for AP2 on the endocytic cargo protein is thought to be necessary for efficient recruitment of the AP2 complex to the plasma membrane (Di Paolo and De Camilli, 2006). Local Arf6 activation by the 3Y motif of GluA2 may therefore promote direct binding of AP2 to GluA2-CT for the formation of AMPAR-containing clathrin-coated pits during LTD. Activated Arf6 may also endow nascent coats with a special protein composition that determines the dynamics and destinations of the resulting endocytic vesicles (Puthenveedu and von Zastrow, 2006). In addition, LTD likely adjusts intracellular sorting of AMPARs into recycling and/or degradation pathways, and Arf6 may play a part here as well.

It is a general question how a receptor to be internalized is coupled to the activation of Arf6 (Paleotti et al., 2005). The direct cooperation between cargo and Arf6-GEF, which we identified here, ensures tight spatial and temporal control over Arf6-mediated coat recruitment. Cargo-mediated stimulation of selected Sec7-domain-containing exchange factors may therefore constitute a widespread cellular mechanism for initiating targeted membrane transport.

EXPERIMENTAL PROCEDURES

Information on reagents, DNA constructs, cell culture, and biochemistry as well as further details of the procedures mentioned below are provided in the Supplemental Information.

Nucleotide Exchange Assay

Arf6 was expressed as described before (Randazzo and Fales, 2002) and myristoylated using plasmid pBB131 (Duronio et al., 1990), which was provided by Dr. Jeffrey Gordon. Nucleotide exchange on Arf6 in vitro was assayed as described (Someya et al., 2001; Venkateswarlu, 2003).

Cellular Arf6-Activation Assay

Arf6 activation in HEK293 cells and cultured rat hippocampal neurons was determined using an $Arf6_{GTP}$-specific pull-down assay (Santy and Casanova, 2001). Immunoblots were quantified using a ChemiDoc RS170 densitometer and Quantity One 4.2 software (Biorad).

Lentiviral Expression

FUGW-based vectors (Dittgen et al., 2004; Lois et al., 2002) for lentiviral expression of short-hairpin RNA constructs and cre recombinase were generated using plasmids provided by Dr. Carlos Lois and Dr. Pavel Osten.

Iqsec1$^{fl/fl}$ Mice

Gene targeting in embryonic stem cells (Nagy et al., 1993) was used to introduce loxP sites flanking exon 2 of the BRAG2 gene *Iqsec1*.

In Vivo Infection of Hippocampal Neurons and Electrophysiology

All animal procedures were in accordance with the animal welfare guidelines of the Max Planck Society. Lentiviral stock was injected into the hippocampus of 3-week-old mice (Dittgen et al., 2004). Two weeks later, acute transverse hippocampal slices were prepared. EPSCs, evoked by Schaffer collateral stimulation every 10 s, were recorded in CA1 neurons in the whole-cell patch-clamp configuration at −70 mV. Comparable amplitudes were obtained with the same range of stimulus intensities in cells with or without manipulation of the BRAG2 level. mGluR-LTD was induced chemically by (*RS*)-3,5-DHPG (10 min, 100 μM, Biotrend), and NMDAR-LTD was induced by LFS (2.5 Hz, 6 min at −50 mV) in presence of mGluR1 antagonist BAY 36-7620 and mGluR5 antagonist MPEP-HCl (20 μM and 10 μM, respectively, Tocris).

Statistical Analysis

All quantitative data are presented as mean ± SEM of at least three independent replicates. A one-tailed Student's t test was applied to calculate statistical differences. The alpha level was set to 0.05.

SUPPLEMENTAL INFORMATION

Supplemental Information includes four figures and Supplemental Experimental Procedures and can be found with this article online at doi:10.1016/j.neuron.2010.05.003.

ACKNOWLEDGMENTS

We thank Julia Kuhlmann, Stefanie Wilhelm, Janina Sülflow, and Sabine Grünewald for excellent technical assistance; Michaela Schweizer for neuronal cultures; Irm Hermans-Borgmeyer for blastocyst injections; Mario Trevino for suggestions on LFS-LTD; Anne Herb and Gisela Eisenhardt for help during

early stages; and Peter H. Seeburg for initial guidance, constant support, and critical reading.

Accepted: April 21, 2010
Published: June 9, 2010

REFERENCES

Ahmadian, G., Ju, W., Liu, L., Wyszynski, M., Lee, S.H., Dunah, A.W., Taghibiglou, C., Wang, Y., Lu, J., Wong, T.P., et al. (2004). Tyrosine phosphorylation of GluR2 is required for insulin-stimulated AMPA receptor endocytosis and LTD. EMBO J. *23*, 1040–1050.

Beattie, E.C., Carroll, R.C., Yu, X., Morishita, W., Yasuda, H., von Zastrow, M., and Malenka, R.C. (2000). Regulation of AMPA receptor endocytosis by a signaling mechanism shared with LTD. Nat. Neurosci. *3*, 1291–1300.

Biou, V., Bhattacharyya, S., and Malenka, R.C. (2008). Endocytosis and recycling of AMPA receptors lacking GluR2/3. Proc. Natl. Acad. Sci. USA *105*, 1038–1043.

Brebner, K., Wong, T.P., Liu, L., Liu, Y., Campsall, P., Gray, S., Phelps, L., Phillips, A.G., and Wang, Y.T. (2005). Nucleus accumbens long-term depression and the expression of behavioral sensitization. Science *310*, 1340–1343.

Chardin, P., Paris, S., Antonny, B., Robineau, S., Béraud-Dufour, S., Jackson, C.L., and Chabre, M. (1996). A human exchange factor for ARF contains Sec7- and pleckstrin-homology domains. Nature *384*, 481–484.

Chen, E.H., Pryce, B.A., Tzeng, J.A., Gonzalez, G.A., and Olson, E.N. (2003). Control of myoblast fusion by a guanine nucleotide exchange factor, loner, and its effector ARF6. Cell *114*, 751–762.

Choi, S., Ko, J., Lee, J.R., Lee, H.W., Kim, K., Chung, H.S., Kim, H., and Kim, E. (2006). ARF6 and EFA6A regulate the development and maintenance of dendritic spines. J. Neurosci. *26*, 4811–4819.

D'Souza-Schorey, C., and Chavrier, P. (2006). ARF proteins: roles in membrane traffic and beyond. Nat. Rev. Mol. Cell Biol. *7*, 347–358.

Derkach, V.A., Oh, M.C., Guire, E.S., and Soderling, T.R. (2007). Regulatory mechanisms of AMPA receptors in synaptic plasticity. Nat. Rev. Neurosci. *8*, 101–113.

Di Paolo, G., and De Camilli, P. (2006). Phosphoinositides in cell regulation and membrane dynamics. Nature *443*, 651–657.

Dittgen, T., Nimmerjahn, A., Komai, S., Licznerski, P., Waters, J., Margrie, T.W., Helmchen, F., Denk, W., Brecht, M., and Osten, P. (2004). Lentivirus-based genetic manipulations of cortical neurons and their optical and electrophysiological monitoring in vivo. Proc. Natl. Acad. Sci. USA *101*, 18206–18211.

Dunphy, J.L., Moravec, R., Ly, K., Lasell, T.K., Melancon, P., and Casanova, J.E. (2006). The Arf6 GEF GEP100/BRAG2 regulates cell adhesion by controlling endocytosis of beta1 integrins. Curr. Biol. *16*, 315–320.

Duronio, R.J., Jackson-Machelski, E., Heuckeroth, R.O., Olins, P.O., Devine, C.S., Yonemoto, W., Slice, L.W., Taylor, S.S., and Gordon, J.I. (1990). Protein N-myristoylation in Escherichia coli: reconstitution of a eukaryotic protein modification in bacteria. Proc. Natl. Acad. Sci. USA *87*, 1506–1510.

Fitzjohn, S.M., Palmer, M.J., May, J.E., Neeson, A., Morris, S.A., and Collingridge, G.L. (2001). A characterisation of long-term depression induced by metabotropic glutamate receptor activation in the rat hippocampus in vitro. J. Physiol. *537*, 421–430.

Fox, C.J., Russell, K., Titterness, A.K., Wang, Y.T., and Christie, B.R. (2007). Tyrosine phosphorylation of the GluR2 subunit is required for long-term depression of synaptic efficacy in young animals in vivo. Hippocampus *17*, 600–605.

Gallo, V., Upson, L.M., Hayes, W.P., Vyklicky, L., Jr., Winters, C.A., and Buonanno, A. (1992). Molecular cloning and development analysis of a new glutamate receptor subunit isoform in cerebellum. J. Neurosci. *12*, 1010–1023.

Gladding, C.M., Collett, V.J., Jia, Z., Bashir, Z.I., Collingridge, G.L., and Molnár, E. (2009). Tyrosine dephosphorylation regulates AMPAR internalisation in mGluR-LTD. Mol. Cell. Neurosci. *40*, 267–279.

Griffiths, S., Scott, H., Glover, C., Bienemann, A., Ghorbel, M.T., Uney, J., Brown, M.W., Warburton, E.C., and Bashir, Z.I. (2008). Expression of long-term depression underlies visual recognition memory. Neuron *58*, 186–194.

Hayashi, T., and Huganir, R.L. (2004). Tyrosine phosphorylation and regulation of the AMPA receptor by SRC family tyrosine kinases. J. Neurosci. *24*, 6152–6160.

Hayashi, T., Umemori, H., Mishina, M., and Yamamoto, T. (1999). The AMPA receptor interacts with and signals through the protein tyrosine kinase Lyn. Nature *397*, 72–76.

Hernández-Deviez, D.J., Casanova, J.E., and Wilson, J.M. (2002). Regulation of dendritic development by the ARF exchange factor ARNO. Nat. Neurosci. *5*, 623–624.

Huang, C.C., and Hsu, K.S. (2006). Sustained activation of metabotropic glutamate receptor 5 and protein tyrosine phosphatases mediate the expression of (S)-3,5-dihydroxyphenylglycine-induced long-term depression in the hippocampal CA1 region. J. Neurochem. *96*, 179–194.

Huber, K.M., Roder, J.C., and Bear, M.F. (2001). Chemical induction of mGluR5- and protein synthesis—dependent long-term depression in hippocampal area CA1. J. Neurophysiol. *86*, 321–325.

Inaba, Y., Tian, Q.B., Okano, A., Zhang, J.P., Sakagami, H., Miyazawa, S., Li, W., Komiyama, A., Inokuchi, K., Kondo, H., and Suzuki, T. (2004). Brain-specific potential guanine nucleotide exchange factor for Arf, synArfGEF (Po), is localized to postsynaptic density. J. Neurochem. *89*, 1347–1357.

Jordan, B.A., Fernholz, B.D., Boussac, M., Xu, C., Grigorean, G., Ziff, E.B., and Neubert, T.A. (2004). Identification and verification of novel rodent postsynaptic density proteins. Mol. Cell. Proteomics *3*, 857–871.

Kastning, K., Kukhtina, V., Kittler, J.T., Chen, G., Pechstein, A., Enders, S., Lee, S.H., Sheng, M., Yan, Z., and Haucke, V. (2007). Molecular determinants for the interaction between AMPA receptors and the clathrin adaptor complex AP-2. Proc. Natl. Acad. Sci. USA *104*, 2991–2996.

Kessels, H.W., and Malinow, R. (2009). Synaptic AMPA receptor plasticity and behavior. Neuron *61*, 340–350.

Klarlund, J.K., Guilherme, A., Holik, J.J., Virbasius, J.V., Chawla, A., and Czech, M.P. (1997). Signaling by phosphoinositide-3,4,5-trisphosphate through proteins containing pleckstrin and Sec7 homology domains. Science *275*, 1927–1930.

Krauss, M., Kinuta, M., Wenk, M.R., De Camilli, P., Takei, K., and Haucke, V. (2003). ARF6 stimulates clathrin/AP-2 recruitment to synaptic membranes by activating phosphatidylinositol phosphate kinase type Igamma. J. Cell Biol. *162*, 113–124.

Lee, S.H., Liu, L., Wang, Y.T., and Sheng, M. (2002). Clathrin adaptor AP2 and NSF interact with overlapping sites of GluR2 and play distinct roles in AMPA receptor trafficking and hippocampal LTD. Neuron *36*, 661–674.

Lee, H.K., Takamiya, K., Han, J.S., Man, H., Kim, C.H., Rumbaugh, G., Yu, S., Ding, L., He, C., Petralia, R.S., et al. (2003). Phosphorylation of the AMPA receptor GluR1 subunit is required for synaptic plasticity and retention of spatial memory. Cell *112*, 631–643.

Lee, H.K., Takamiya, K., He, K., Song, L., and Huganir, R.L. (2010). Specific roles of AMPA receptor subunit GluR1 (GluA1) phosphorylation sites in regulating synaptic plasticity in the CA1 region of hippocampus. J. Neurophysiol. *103*, 479–489.

Lin, J.W., Ju, W., Foster, K., Lee, S.H., Ahmadian, G., Wyszynski, M., Wang, Y.T., and Sheng, M. (2000). Distinct molecular mechanisms and divergent endocytotic pathways of AMPA receptor internalization. Nat. Neurosci. *3*, 1282–1290.

Lois, C., Hong, E.J., Pease, S., Brown, E.J., and Baltimore, D. (2002). Germline transmission and tissue-specific expression of transgenes delivered by lentiviral vectors. Science *295*, 868–872.

Lu, W., Shi, Y., Jackson, A.C., Bjorgan, K., During, M.J., Sprengel, R., Seeburg, P.H., and Nicoll, R.A. (2009). Subunit composition of synaptic AMPA receptors revealed by a single-cell genetic approach. Neuron *62*, 254–268.

Macia, E., Luton, F., Partisani, M., Cherfils, J., Chardin, P., and Franco, M. (2004). The GDP-bound form of Arf6 is located at the plasma membrane. J. Cell Sci. *117*, 2389–2398.

Malenka, R.C., and Bear, M.F. (2004). LTP and LTD: an embarrassment of riches. Neuron *44*, 5–21.

Man, H.Y., Lin, J.W., Ju, W.H., Ahmadian, G., Liu, L., Becker, L.E., Sheng, M., and Wang, Y.T. (2000). Regulation of AMPA receptor-mediated synaptic transmission by clathrin-dependent receptor internalization. Neuron *25*, 649–662.

Massey, P.V., and Bashir, Z.I. (2007). Long-term depression: multiple forms and implications for brain function. Trends Neurosci. *30*, 176–184.

Meng, Y., Zhang, Y., and Jia, Z. (2003). Synaptic transmission and plasticity in the absence of AMPA glutamate receptor GluR2 and GluR3. Neuron *39*, 163–176.

Menuz, K., Stroud, R.M., Nicoll, R.A., and Hays, F.A. (2007). TARP auxiliary subunits switch AMPA receptor antagonists into partial agonists. Science *318*, 815–817.

Morishige, M., Hashimoto, S., Ogawa, E., Toda, Y., Kotani, H., Hirose, M., Wei, S., Hashimoto, A., Yamada, A., Yano, H., et al. (2008). GEP100 links epidermal growth factor receptor signalling to Arf6 activation to induce breast cancer invasion. Nat. Cell Biol. *10*, 85–92.

Moult, P.R., Gladding, C.M., Sanderson, T.M., Fitzjohn, S.M., Bashir, Z.I., Molnar, E., and Collingridge, G.L. (2006). Tyrosine phosphatases regulate AMPA receptor trafficking during metabotropic glutamate receptor-mediated long-term depression. J. Neurosci. *26*, 2544–2554.

Moult, P.R., Corrêa, S.A., Collingridge, G.L., Fitzjohn, S.M., and Bashir, Z.I. (2008). Co-activation of p38 mitogen-activated protein kinase and protein tyrosine phosphatase underlies metabotropic glutamate receptor-dependent long-term depression. J. Physiol. *586*, 2499–2510.

Munton, R.P., Tweedie-Cullen, R., Livingstone-Zatchej, M., Weinandy, F., Waidelich, M., Longo, D., Gehrig, P., Potthast, F., Rutishauser, D., Gerrits, B., et al. (2007). Qualitative and quantitative analyses of protein phosphorylation in naive and stimulated mouse synaptosomal preparations. Mol. Cell. Proteomics *6*, 283–293.

Murphy, J.A., Jensen, O.N., and Walikonis, R.S. (2006). BRAG1, a Sec7 domain-containing protein, is a component of the postsynaptic density of excitatory synapses. Brain Res. *1120*, 35–45.

Nagy, A., Rossant, J., Nagy, R., Abramow-Newerly, W., and Roder, J.C. (1993). Derivation of completely cell culture-derived mice from early-passage embryonic stem cells. Proc. Natl. Acad. Sci. USA *90*, 8424–8428.

Newpher, T.M., and Ehlers, M.D. (2008). Glutamate receptor dynamics in dendritic microdomains. Neuron *58*, 472–497.

Nicoll, R.A., Oliet, S.H., and Malenka, R.C. (1998). NMDA receptor-dependent and metabotropic glutamate receptor-dependent forms of long-term depression coexist in CA1 hippocampal pyramidal cells. Neurobiol. Learn. Mem. *70*, 62–72.

Oliet, S.H., Malenka, R.C., and Nicoll, R.A. (1997). Two distinct forms of long-term depression coexist in CA1 hippocampal pyramidal cells. Neuron *18*, 969–982.

Pajcini, K.V., Pomerantz, J.H., Alkan, O., Doyonnas, R., and Blau, H.M. (2008). Myoblasts and macrophages share molecular components that contribute to cell-cell fusion. J. Cell Biol. *180*, 1005–1019.

Paleotti, O., Macia, E., Luton, F., Klein, S., Partisani, M., Chardin, P., Kirchhausen, T., and Franco, M. (2005). The small G-protein Arf6GTP recruits the AP-2 adaptor complex to membranes. J. Biol. Chem. *280*, 21661–21666.

Palmer, M.J., Irving, A.J., Seabrook, G.R., Jane, D.E., and Collingridge, G.L. (1997). The group I mGlu receptor agonist DHPG induces a novel form of LTD in the CA1 region of the hippocampus. Neuropharmacology *36*, 1517–1532.

Peng, J., Kim, M.J., Cheng, D., Duong, D.M., Gygi, S.P., and Sheng, M. (2004). Semiquantitative proteomic analysis of rat forebrain postsynaptic density fractions by mass spectrometry. J. Biol. Chem. *279*, 21003–21011.

Puthenveedu, M.A., and von Zastrow, M. (2006). Cargo regulates clathrin-coated pit dynamics. Cell *127*, 113–124.

Randazzo, P.A., and Fales, H.M. (2002). Preparation of myristoylated Arf1 and Arf6 proteins. Methods Mol. Biol. *189*, 169–179.

Santy, L.C., and Casanova, J.E. (2001). Activation of ARF6 by ARNO stimulates epithelial cell migration through downstream activation of both Rac1 and phospholipase D. J. Cell Biol. *154*, 599–610.

Shepherd, J.D., and Huganir, R.L. (2007). The cell biology of synaptic plasticity: AMPA receptor trafficking. Annu. Rev. Cell Dev. Biol. *23*, 613–643.

Snyder, E.M., Philpot, B.D., Huber, K.M., Dong, X., Fallon, J.R., and Bear, M.F. (2001). Internalization of ionotropic glutamate receptors in response to mGluR activation. Nat. Neurosci. *4*, 1079–1085.

Someya, A., Sata, M., Takeda, K., Pacheco-Rodriguez, G., Ferrans, V.J., Moss, J., and Vaughan, M. (2001). ARF-GEP(100), a guanine nucleotide-exchange protein for ADP-ribosylation factor 6. Proc. Natl. Acad. Sci. USA *98*, 2413–2418.

Van den Oever, M.C., Goriounova, N.A., Li, K.W., Van der Schors, R.C., Binnekade, R., Schoffelmeer, A.N., Mansvelder, H.D., Smit, A.B., Spijker, S., and De Vries, T.J. (2008). Prefrontal cortex AMPA receptor plasticity is crucial for cue-induced relapse to heroin-seeking. Nat. Neurosci. *11*, 1053–1058.

Venkateswarlu, K. (2003). Interaction protein for cytohesin exchange factors 1 (IPCEF1) binds cytohesin 2 and modifies its activity. J. Biol. Chem. *278*, 43460–43469.

Waung, M.W., Pfeiffer, B.E., Nosyreva, E.D., Ronesi, J.A., and Huber, K.M. (2008). Rapid translation of Arc/Arg3.1 selectively mediates mGluR-dependent LTD through persistent increases in AMPAR endocytosis rate. Neuron *59*, 84–97.

Wong, T.P., Howland, J.G., Robillard, J.M., Ge, Y., Yu, W., Titterness, A.K., Brebner, K., Liu, L., Weinberg, J., Christie, B.R., et al. (2007). Hippocampal long-term depression mediates acute stress-induced spatial memory retrieval impairment. Proc. Natl. Acad. Sci. USA *104*, 11471–11476.

Xiao, M.Y., Zhou, Q., and Nicoll, R.A. (2001). Metabotropic glutamate receptor activation causes a rapid redistribution of AMPA receptors. Neuropharmacology *41*, 664–671.

Yu, S.Y., Wu, D.C., Liu, L., Ge, Y., and Wang, Y.T. (2008). Role of AMPA receptor trafficking in NMDA receptor-dependent synaptic plasticity in the rat lateral amygdala. J. Neurochem. *106*, 889–899.